LA-UR- 10-07989

Approved for public release; distribution is unlimited.

Title: On Specification of Initial Conditions in Turbulence Models

Author(s): Bertrand Rollin
Malcolm J. Andrews

Intended for: Proceedings of the 12th International Workshop on the Physics of Compressible Turbulent Mixing (IWPCTM12)

Los Alamos NATIONAL LABORATORY EST. 1943

On Specification of Initial Conditions in Turbulence Models

Bertrand Rollin & **Malcolm J. Andrews**

Los Alamos National Laboratory
bertrand@lanl.gov

Abstract

Recent research has shown that initial conditions have a significant influence on the evolution of a flow towards turbulence. This important finding offers a unique opportunity for turbulence control, but also raises the question of how to properly specify initial conditions in turbulence models. We study this problem in the context of the Rayleigh-Taylor instability. The Rayleigh-Taylor instability is an interfacial fluid instability that leads to turbulence and turbulent mixing. It occurs when a light fluid is accelerated in to a heavy fluid because of misalignment between density and pressure gradients. The Rayleigh-Taylor instability plays a key role in a wide variety of natural and man-made flows ranging from supernovae to the implosion phase of Inertial Confinement Fusion (ICF). Our approach consists of providing the turbulence models with a predicted profile of its key variables at the appropriate time in accordance to the initial conditions of the problem.

Nomenclature

RT	Rayleigh-Taylor
A	Atwood number
ICF	Inertial Confinement Fusion
ODE	Ordinary Differential Equation
k	wavenumber
g	gravity
TMZ	Turbulence Mixing Zone (zone between the bubbles and spikes fronts)

Introduction

The RT instability [1, 2] occurs when a perturbation is introduced at the interface between two media in a configuration such that the pressure gradient opposes the density gradient. One common situation is when a heavy fluid sits on top a light fluid in the gravitational field. At early time, the perturbation's amplitude grows exponentially. Then, significant non-linearities appear as vorticity is generated by a baroclinic mechanism. Finally, the two fluids mix in a turbulent fashion. This instability is characterized by the Atwood number, $A = (\rho_h - \rho_l)/(\rho_h + \rho_l)$, which describes the density contrast between the two fluids. Recent research [3, 4] has shown that initial conditions have a significant influence on the evolution of the turbulent RT instability. This characteristic offers an opportunity for "turbulence control", which may result in significant optimization for engineering applications such as ICF [5] or heat exchangers and sprays in internal combustors [6]. Because traditional turbulence models used for simulating these complex problems do not capture initial conditions effects, our objective is to define a rational basis for "feeding" them with initial variables values that reflect initial conditions' influence. In the next section, we describe our model for RT TMZ growth. Then, we discuss the case of a complex multi-band initial perturbation spectrum. Finally, we briefly describe our method for defining profiles of turbulence model variables.

Mixing Zone Evolution

Our current model for RT mixing zone evolution is based on Goncharov's model [7] for single mode perturbations. The Goncharov model is an extension of Layzer's potential flow theory [8] for arbitrary Atwood numbers. In a three-dimensional axisymmetric geometry, the interface between the two-fluids at the tip of the perturbation is approximated by:

$$\eta(x,t)=\eta_0(t)+\eta_2(t)r^2 \tag{1}$$

where η_0 is the perturbation's amplitude, and η_2 is related to the perturbation's curvature. In potential flow theory, the assumption is made that the fluids are irrotational in the vicinity of the perturbation's tip. One can then define velocity potentials [7] that are used in the equations describing the conditions at the fluids' interface. The expansion of these equations to the second order provides a set of ODE governing the dynamics of

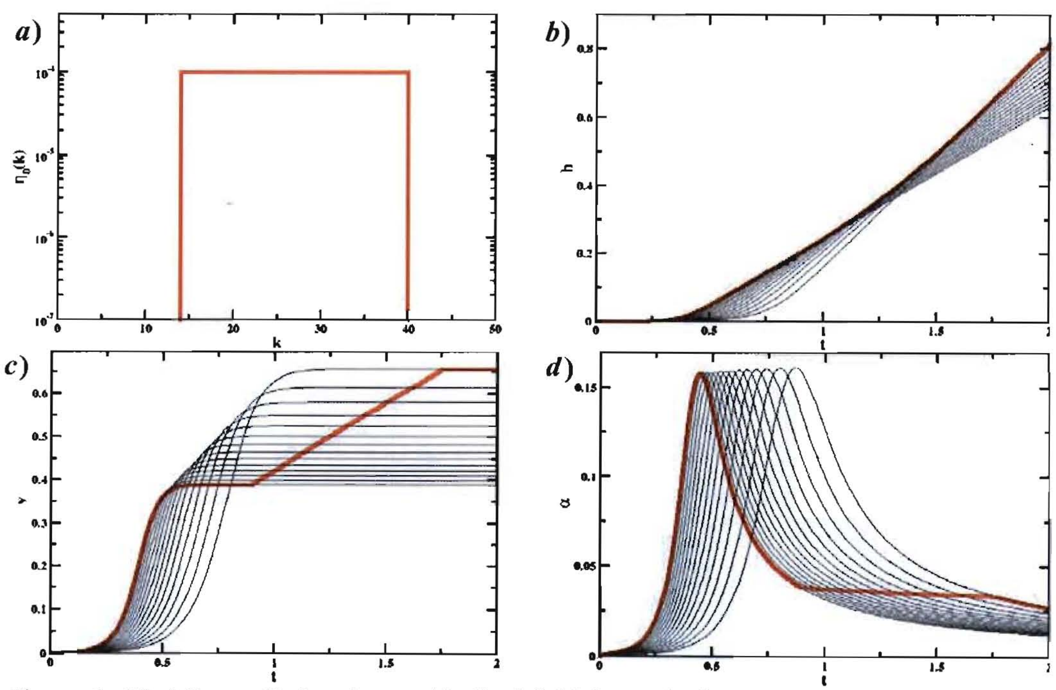

Figure 1: Model's prediction for an idealized initial amplitude spectrum. a) initial amplitude spectrum; b) height, c) velocity, and d) growth rate as a function of time. Bold red line: bubbles' front. Light black lines: single mode bubbles

the tip of the RT perturbation until relatively late in the nonlinear regime. For the bubble's dynamics, the set of ODE is:

$$\dot{\eta}_2 = -\dot{\eta}_0 \frac{k}{2}(k + 8\eta_2) \tag{2}$$

$$\alpha_1 \ddot{\eta}_0 + \alpha_2 \dot{\eta}_0^2 + Ag\eta_2 = 0 \tag{3}$$

where $\alpha_1 = \dfrac{k^2 - 4Ak\eta_2 - 32A\eta_2^2}{4(k - 8\eta_2)}$ and $\alpha_2 = k^2 \dfrac{(5A-4)k^2 + 16(2A-3)k\eta_2 + 64A\eta_2^2}{8(k - 8\eta_2)^2}$.

The set of equations governing the dynamics of the tip of the RT spike is obtained from equations $(2)-(3)$ by substituting $\eta \to -\eta$, $A \to -A$, and $g \to -g$. This nonlinear model captures with some success the penetration of the bubble for $0 \le A \le 1$, but fails to predict accurately the penetration of the spike for $A \ge 0.4$ [7].

For our multimode model, we compute the evolution of every existing modes of the initial perturbation spectrum. The evolution of the bubbles (spikes) front then is given by the envelope of the single modes heights at all times:

$$h(t) = \max_k (h_k(t)) \tag{4}$$

where $h(t)$ is the height of the bubbles (spikes) front at time t and $h_k(t) = |\eta_{0,k}(t) - \eta_{0,k}(0)|$ is the height of the bubble (spike) generated by a single mode initial perturbation at time t. The bubbles (spikes) front's velocity is $v = dh/dt$, and the bubbles (spikes) front growth rate is $\alpha = \dot{h}^2/4Agh$ [9].

Figure 1 illustrates how our multimode model behaves on an idealized case. Figure 1a displays an initial amplitude spectrum that could result from azimuthally averaging the two-dimensional spectrum of an initial perturbation interface. Figure 1b shows the height of the bubble front, bold red line, as a function of time as well as the height of a number of single modes, light black lines. Using the same color code as in figure 1b, figure 1c shows the velocity, and figure 1d shows the growth rate. Since we consider an ideal case, without viscosity or surface tension, the fastest growing mode is the largest mode. As figures 1c and 1d clearly show, the largest mode is the dominant mode until $t \approx 0.8s$. Until then, the front grows as a single mode bubble. Then, between $t \approx 0.8s$ and $t \approx 1.75s$, smaller and smaller modes lead the bubbles front subsequently. The natural

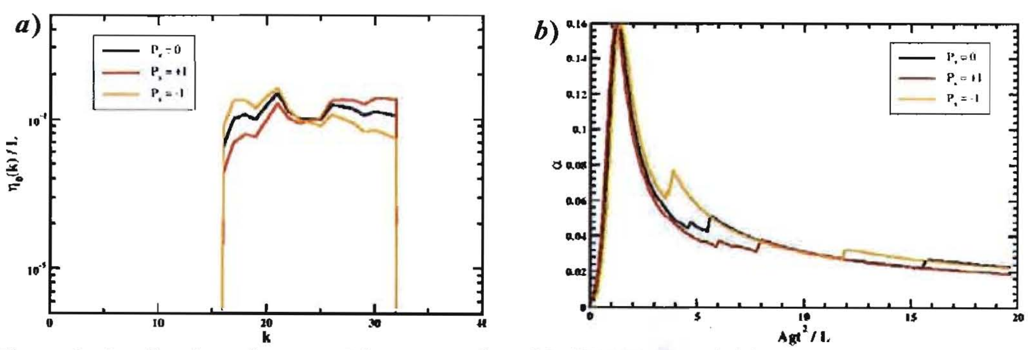

Figure 2: Application of our model to a case found in literature. a) initial amplitude spectra used by Banerjee and Andrews. b) Growth rate predicted by our model, to be compared with figure 10 of Banerjee and Andrews [4]

pace at which the modes relay each other in leading the front produces a quadratic evolution in time. As a result, the growth rate, figure 1d reaches an asymptotic value of about $\mathbf{0.03}$. Finally, the growth rate decays slowly between $t \approx 1.75s$ and the end of the run. This decay is due to "missing" modes in our run. Since our model does not handle mode coupling, there is also no mode generation. As the dominant mode in our simulation is smaller and smaller, our model eventually "runs out" of modes and the bubble front is lead by the smallest mode available in our initial spectrum. Since the terminal velocity of a single mode is constant, its height then grows linearly, and its growth rate decays as an inverse function of time. Figure 1 shows that our model can reproduce the evolution of a multimode bubbles (spikes) front, but is limited by its inability to generate modes. Figure 2 reproduces the spectral index study made by Banerjee and Andrews [4], with our multimode model. Their MILES simulations predict a late time growth rate of $\alpha \approx 0.02-0.03$, as does our multimode without mode coupling. This figure illustrates how, for simply structured spectra, our model provides a reasonable prediction of the late time growth rate, as long as the initial amplitude spectrum is sufficiently wide.

Complex Initial Perturbation Spectrum

One argument used to explain larger growth rates obtained in experiments, in comparison to values obtained in simulations, is the presence in the initial conditions of parasitic long wavelengths in addition to the short wavelength intended by the experimentalists. Simulations of this type of banded initial perturbation spectrum have been performed by Banerjee and Andrews [4]. Their results showed that the long wavelength will produce an "anomaly" during the growth of the mixing layer. Figure 3 shows an example of banded initial perturbation spectrum and the resulting mixing layer growth rate. The evolution of the growth rate suggests that, at first, short wavelengths lead the mixing layer expansion and the front achieve the quadratic evolution in time. Then, the long wavelengths that have a smaller initial growth rate, but a larger saturation velocity, eventually catch up with the front of the mixing layer and accelerate the growth for a short period of time. This is characterized by a relatively significant secondary peak at $t = T_A$ on figure 3b. Eventually, the mixing layer returns to a self-similar growth.

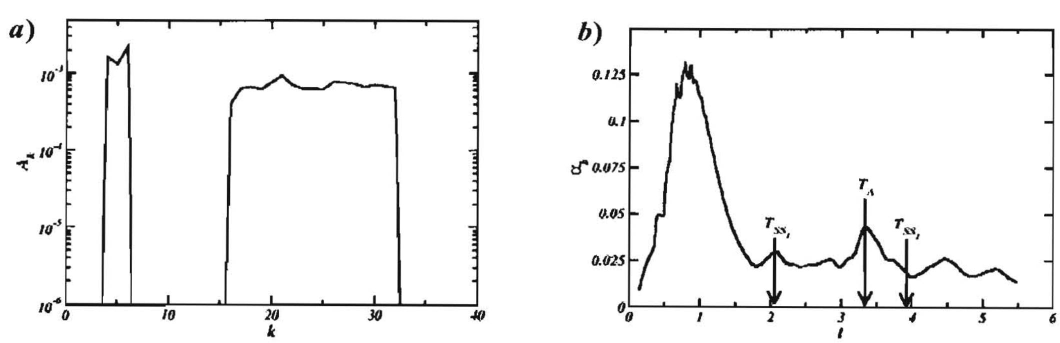

Figure 3: Behavior of a banded spectrum. a) Initial perturbation spectrum. b) growth rate obtained by MILES simulation. T_A: time of anomalie; T_{SS1}: first time of self-similarity growth; T_{SS2}: time of return to self-similarity growth

This type of anomaly needs to be predicted in order to "inform" the turbulence model that for a given period of time, the growth rate will not be constant. Four quantities need to be known: the time at which the growth of the front first become self-similar, T_{SS1}, the time at which an anomaly occur if it is to occur, T_A, and the resulting growth rate, α_A, and the time at which the growth becomes self-similar again, T_{SS2}. A direct estimate from the initial spectrum is possible, following the same approach as in our multimode model. A short period of time after the fastest growing mode has saturated, the leading mode in the front of the mixing layer is a saturated mode. One can then approximate the height of each mode at a given time by computing:

$$h_k(t) = V_k^{\infty}\left(t - t_k^{NL}\right) + h_k^{NL} \qquad (5)$$

where $V_k^{\infty} = \sqrt{2Ag/(1+A)k}$, $t_k^{NL} = \left(1/\sqrt{Agk}\right)\sinh^{-1}\left(V_k^{\infty}/h_k(0)\sqrt{Agk}\right)$, and $h_k^{NL} = h_k(0)\cosh\left(t_k^{NL}\sqrt{Agk}\right)$. The height of the front is then the largest computed height, and the front velocity is the saturation velocity of the mode having the largest height. Figure 4 shows an idealized banded spectrum (figure 4a) and a comparison of prediction of growth rate (figure 4b) using our ODE multimode model and the direct approach described above. One can see on figure 4b that the direct approach (red dots) gives a reasonable prediction of T_{SS1}, T_A, α_A, and T_{SS2} in comparison with the ODE multimode model (solid line).

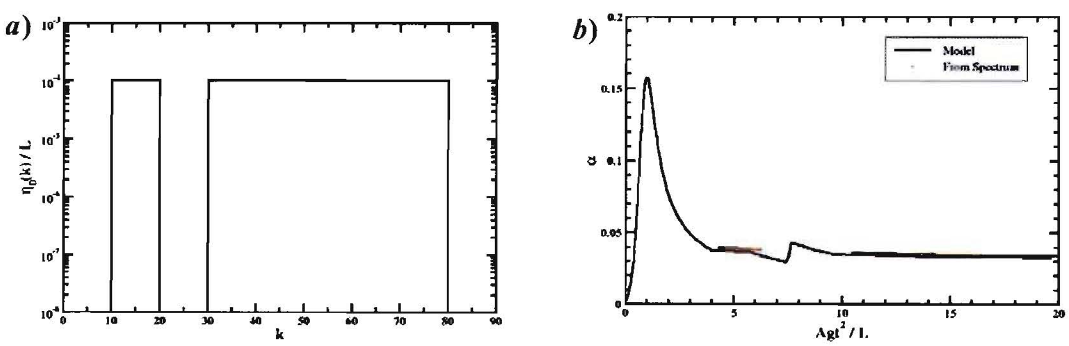

Figure 4: Direct prediction of TMZ growth without solving ODEs. a) Idealized initial banded perturbation spectrum. b) Growth rate obtained by direct prediction (red dots), and ODE multimode model (solid black line)

Turbulence Variable Modeling

Using the ODE multimode model, or the direct prediction model describe in previous sections, the turbulence model user can make an informed decision on an appropriate time to start his model, and knows the basic characteristics of the TMZ (fronts positions and velocities) at that time. He then needs information on the turbulence model variables.

We extract turbulence variables' profiles using a two-fluid model [10].The model is based on an idealization of the mixing interface between two interpenetrating fluids. Assuming a linear distribution of the mixture fraction within the TMZ [11, 12], the averaged density and velocity at a given altitude z are given by:

$$\bar{\rho}(z) = f_h(z)\rho_h + f_l(z)\rho_l \qquad (6)$$

$$\overline{u}_z(z) = f_h(z)u_h + f_l(z)u_l \quad (7)$$

where $\rho_{h/l}$ is the heavy/light density and $f_{h/l}$ is the heavy/light volume fraction. Fluctuating quantities at a given altitude are then computed using averages given by equations (6), or (7), and bulk values for the heavy fluid or the light fluid [10]. Upon substitution of the appropriate terms in the definition of a turbulence variable, one gets a two-fluid expression for its profile. For example, a two-fluid formulation for the mass flux, $a_z = \overline{\rho' u'_z}/\overline{\rho}$, is:

$$a_z(z) = \frac{f_h(z) f_l(z)}{f_h(z)\rho_h + f_l(z)\rho_l}(\rho_h - \rho_l)(|v_s| + |v_b|) \quad (8)$$

Conclusions

We presented our current approach for introducing initial conditions effects in turbulence models for RT instability. In a first time, we use a modal model to predict the evolution of the TMZ. In spite of the lack of mode coupling, our model captures reasonably well the growth of the TMZ as long as the initial perturbation spectrum is wide enough. In case of a complex initial perturbation spectrum, our model, or a direct prediction model, can be used to estimate times of occurrence for key features of the TMZ growth. Then, profiles of turbulence variables are computed by using the characteristics of the TMZ, and a two-fluid model. In the future, our predictions will be refined by using a multimode model that includes mode coupling, and complimentary studies will be made on the turbulence in the TMZ to characterize the initial time of validity for the turbulence model hypotheses.

Acknowledgment

This work is funded by the Laboratory Directed Research and Development Program at Los Alamos National Laboratory through directed research project number LDRD-20090058DR.

References

[1] Lord Rayleigh, Proc. Lond. Math. Soc., **14**, 170–177 (188 3).
[2] Taylor G.I., Proc. Royal. Soc. Lond. A, **201**, 192-196 (1950).
[3] P. Ramaprabhu, G. Dimonte and M. J. Andrews, J. Fluid Mech., **536**, 285-319 (2005).
[4] A. Banerjee & M. J. Andrews, Intl. J. Heat and Mass Transfer **52**, 3906-3917 (2009).
[5] Roberts P.D., Rose S.J., Thompson P.C., and Wright, R.J., Vol. 13, pp. 1980 (1957).
[6] Beale J.C. and Ritz R.D., *Atomiz. Sprays*, Vol. 9, pp. 623-650 (1999).
[7] V.N. Goncharov, Phys. Rev. Lett., 88, 1234502 (2002).
[8] D. Layzer, Astrophys. J., **122**, 1 (1955).
[9] J. R. Ristorcelli and T. T. Clark, J. Fluid Mech., **57**, 213-253 (2004).
[10] B. Rollin & M. J. Andrews, in Proceedings of ASME, FEDSM-ICNMM2010-30556
[11] [17] G. Dimonte *etal.*, Phys. of Fluids, **16**, 5 (2004)
[12] D. Livescu *et al.*, J. Turbulence, **10**, 13, 1-32 (2009).